Alexandria Engineering Journal (2021) 60, 2127–2137

HOSTED BY

ELSEVIER

Alexandria University

Alexandria Engineering Journal

www.elsevier.com/locate/aej
www.sciencedirect.com

# Numerical and scale analysis of non-Newtonian fluid (Eyring-Powell) through pseudo-spectral collocation method (PSCM) towards a magnetized stretchable Riga surface

**Yu-Ming Chu [a,b], Fayyaz Ahmad [c], M. Ijaz Khan [d,*], Mubbashar Nazeer [e], Farooq Hussain [f], Niaz B. Khan [g], S. Kadry [h], Liquan Mei [i]**

[a] *Department of Mathematics, Huzhou University, Huzhou 313000, PR China*
[b] *Hunan Provincial Key Laboratory of Mathematical Modeling and Analysis in Engineering, Changsha University of Science & Technology, Changsha 410114, PR China*
[c] *Department of Applied Sciences, National Textile University Faisalabad, Pakistan*
[d] *Department of Mathematics and Statistics, Riphah International University, I-14, Islamabad 44000, Pakistan*
[e] *Department of Mathematics, Institute of Arts and Science, Government College University Faisalabad, Chiniot Campus, Pakistan*
[f] *Department of Mathematical Sciences (FABS) BUITEMS, Quetta 87300, Pakistan*
[g] *School of Mechanical and Manufacturing Engineering, National University of Sciences and Technology, Islamabad, Pakistan*
[h] *Department of Mathematics and Computer Science, Beirut Arab University, Beirut, Lebanon*
[i] *School of Mathematics and Statistics, Xi'an Jiaotong University, Xi'an, Shaanxi 710049, PR China*

Received 21 September 2020; revised 21 October 2020; accepted 16 December 2020
Available online 31 December 2020

**KEYWORDS**

Mixed convection flow;
Heat transfer;
Sherwood number;
Pseudo-spectral method;
Riga plate

**Abstract** A numerical simulation of a two-dimensional Eyring-Powell nanofluid flow is carried out through a Riga plate with radiative walls. Simultaneous contributions of chemical reaction and activation energy have also been taken into account on the mixed convection flow. Lubrication effects are applied by considering second order slip boundary condition in order to reduce the role of skin friction. A set of highly nonlinear and coupled differential equations are tackled with the help of *"Pseudo-spectral collocation method"* by developing numerical code on MATLAB. A detailed parametric study is performed that reveals that more energy adds to the system in response to slip parameter and Brownian motion of the nano-particles. Numerical results have also been compiled and tabulated. This is worth noticing that skin friction coefficient reduces due to modified Hartmann factor while heat flux is an increasing function of Prandtl number. However, there is a prominent increase in mass flux against all parameter, except activation energy.



* Corresponding author.
E-mail address: ijazfmg_khan@yahoo.com (M.I. Khan).

Peer review under responsibility of Faculty of Engineering, Alexandria University.

https://doi.org/10.1016/j.aej.2020.12.017
1110-0168

## 1. Introduction

Non-Newtonian fluids have broader features as compared to Newtonian fluid. For such fluids demonstrate solid and liquids properties, besides, a highly nonlinear relationship between shear stress and shear rate. Therefore, such fluids have a frequent use in the industrial and technological processes. Many prominent research endeavors from the exiting literature, can be cited which analyze of such behaviors of non-Newtonian fluids [1–10], including Powell-Eyring fluid model and some other fluid models [11–15], on stretching surfaces having different configurations. Seyedi et al. [16] used the spectral numerical method for non-Newtonian flow of Eyring Powell fluid bounded within stretching walls. The numerical solution obtained by the spectral method is validated with the help of another numerical technique i.e., Runge-Kutta method. The comparison shows that both numerical solutions are in good agreement. They maintained that squeezing number results to accelerate temperature, velocity and concentration profiles. Nanofluid flow of an Eyring Powell fluid over a Riga surface is investigated by Rasool and Zhang [17]. Natural convection is the main contributor of bi-phase flow. The effects of magnetic field, thermal radiation and convective boundary conditions are also incorporated which impart a significant impact on physical quantities. They conclude that the efficiency in the flow and heat transfer is enhanced by suspension of the nanoparticles. Bhatti et al. [18] provide an approximate solution for a non-Newtonian flow caused by the expansion of the flat surface. Again, the main carries are Eyring-Powell which undergoes the effects of entropy generation. Besides, graphics numerical results have also been tabulated that describe the contribution of main parameters such as, Nusselt number and Sherwood number, in particular.

The magnetic field plays an integral role in fluid mechanics due to its vast application to increase the thermo-physical behavior of the fluid. Fields namely, earth sciences and astrology etc. encounter various type of fluids which are not good conductors of the electricity. In this situation, the external factor is always required to increase the heat transfer mechanism with superior conductivity and other associated thermo-physical properties. The external factor may be a magnetic bar or permanently group of such magnets with alternating electrodes. Such agents were brought under consideration by Gailitis and Lielausis [19] and named as Riga plate. The configuration of Riga plate makes it demanding in short span of time that earned the its' use in industrial and engineering processes including fluid flow phenomenon. Bhatti et al. [20] have considered Riga surface for electrohydrodynamics (EHD). The numerical solution obtained with the help of shooting technique features that nanoparticle, play a highly supportive role in heat enhancement. Similarly, Abbas et al. [21–22] focus on nanofluid flows through Riga respectively, porous and non-porous surfaces, numerically. The flow of viscous nanofluid under the account of entropy generation is tackled by using shooting method.

Recent developments show that nano-sized metallic particles are in frequent use in various industrial and engineering processes. Such particles are added in various types of fluid which help to enhance thermal conductivity. The reason for choosing micro level particles suggests that these easily suspend in any base liquid well, as compared to larger particles. Various significant applications in the list [23–25] have been reported by renowned researchers that highlight the use of tiny particles such as, micro production, ventilation, chemical processes, power generation, heating and cooling etc. Krishna and Chamkha [26–27] discussed the boundary layer flow of nanofluid under the effects of Hall and ion slip through a rotating disc and presented some important results. Chamkha et al. [28] considered the single and double nanoparticles to highlight the phase-changing material through a square closed enclosure that heats up a circular cylinder at the middle part of the conduit. The numerical solution was obtained by using the finite element method and constructed the graphs in term of contours.

In view of diverse applications of nanofluid and Riga surfaces, the exiting literature suggests that no attention has been given to mixed convection flows through the concerned geometry. The only existing evidence pertains to natural convection flow of Eyring-Powell. However, no noteworthy research can be reported which addresses beyond the presented theoretical analysis. Therefore, this manuscript deals with the Eyring-Powell fluid suspended with nano particles through Riga surface. Besides, the suspension of nano particles, contribution of activation energy has been incorporated in order to improve thermo-physical properties of nanofluid. System of nonlinear differential equations is solved numerical by using pseudo-spectral collocation method and a detailed parametric study is carried out Eyring-Powell nanofluid under the influence of thermal radiation and viscous dissipation.

## 2. Mathematical formulation

We have considered the mixed convection flow of an Eyring-Powell nanofluid through a Riga surface. We also assumed the thermal conductivity and viscous is not varying with respect to temperature of pressure. The convective boundary conditions of heat and mass transfer are also taken. The governing equations in term of partial differential equations are given by

$$\frac{\partial u}{\partial x}+\frac{\partial v}{\partial y}=0 \tag{1}$$

$$\begin{aligned} u\frac{\partial u}{\partial x}+v\frac{\partial u}{\partial y} &= \left(\nu+\frac{1}{\rho_f\gamma C^*}\right)\frac{\partial^2 u}{\partial y^2}-\frac{1}{2\rho_f\gamma C^{*3}}\left(\frac{\partial u}{\partial y}\right)^2\frac{\partial^2 u}{\partial y^2} \\ &+\left(\frac{\pi j_o M_o}{8\rho_l}\right)\exp\left[\frac{-\pi y}{b}\right]+g\begin{pmatrix}\beta_1(T-T_\infty)+\beta_2(T-T_\infty)^2\\ +\beta_3(C-C_\infty)+\beta_4(C-C_\infty)^2\end{pmatrix}, \end{aligned} \tag{2}$$

$$\begin{aligned} u\frac{\partial T}{\partial x}+v\frac{\partial T}{\partial y} &= \alpha\frac{\partial^2 T}{\partial y^2}+\tau\left(D_B\frac{\partial T}{\partial y}\frac{\partial C}{\partial y}+\frac{D_T}{T_\infty}\left(\frac{\partial T}{\partial y}\right)^2\right) \\ &+\frac{1}{(\rho c)_l}\frac{16\sigma^* T_\infty^3}{3K^*}\left(\frac{\partial^2 T}{\partial y^2}\right), \end{aligned} \tag{3}$$

$$\begin{aligned} u\frac{\partial C}{\partial x}+v\frac{\partial C}{\partial y} &= D_B\frac{\partial^2 C}{\partial y^2}+\frac{D_T}{T_\infty}\frac{\partial^2 T}{\partial y^2} \\ &-K_r^2(C-C_\infty)\left(\frac{T}{T_\infty}\right)^n\exp\left(\frac{-E_a}{KT}\right). \end{aligned} \tag{4}$$

The boundary conditions of the consider problem is given by

$$u = ax + \lambda_i \left[ \left( 1 + \frac{1}{\mu_f \gamma C^{*2}} \right) \frac{\partial u}{\partial y} - \frac{1}{\mu_f \gamma C^{*3}} \left( \frac{\partial u}{\partial y} \right)^3 \right],$$

$$v = 0, -K\frac{\partial T}{\partial y} = h_1^*(T_a - T), -D_B\frac{\partial C}{\partial y} = h_2^*\left(C_{np} - C\right).\text{at } y = 0$$

$$u \to 0, T \to T_\infty, C \to C_\infty \quad \text{at} \quad y \to \infty \tag{5}$$

The dimensional form of important physical quantities is defined as

$$C_f = \frac{2\tau_w}{\rho_f U_w^2}, \tau_w = \left[ \left( \mu_{nf} + \frac{1}{\gamma C^*} \right) \frac{\partial u}{\partial y} - \frac{1}{6\gamma C^{*3}} \left( \frac{\partial u}{\partial y} \right)^3 \right], \tag{7}$$

$$Nu_x = \frac{xq_w}{K(T_l - T_\infty)}, q_w = -K\frac{\partial T}{\partial y} - \frac{16\sigma^* T_\infty^3}{3K^*}\frac{\partial T}{\partial y}, \tag{8}$$

$$Sh_x = \frac{xq_m}{D_B\left(C_{np} - C_\infty\right)}, q_w = -D_B\frac{\partial C}{\partial y}. \tag{9}$$

Define the following transformation

$$u = axf', v = -\sqrt{a\nu}f, \eta = \sqrt{\frac{a}{\nu}}y, \theta = \frac{T - T_\infty}{T_l - T_\infty}, \phi = \frac{C - C_\infty}{C_{np} - C_\infty}. \tag{7}$$

The non-dimension form with boundary conditions is given by

$$(1+k)f''' - \frac{1}{3}\mathrm{K}\Lambda f''^2 f''' + ff'' - f'^2 + Q\exp(-\beta\eta)$$
$$+ \lambda\theta(1 + \beta_t\theta) + \lambda\mathrm{N}^*\phi(1 + \beta_c\phi) = 0, \tag{8}$$

$$\left(1 + \frac{4}{3}Rd\right)\theta'' + \Pr(\mathrm{N}b\theta'\phi' + f\theta' + \mathrm{N}t\theta'^2) = 0, \tag{9}$$

$$\phi'' + Le\Pr\left(f\phi' - k_1\phi(1+\delta\theta)^n\exp\left(\frac{-E_1}{(1+\delta\theta)}\right)\right) + \frac{\mathrm{N}t}{\mathrm{N}b}\theta'' = 0, \tag{10}$$

$$f'(0) = 1 + L_1\left((1+k)f''(0) - \frac{1}{3}\mathrm{K}\Lambda(f''(0))^3\right), \tag{11}$$

$$f(0) = 0, \theta'(0) = -\alpha_1(1 - \theta(0)), \phi'(0) = -\alpha_2(1 - \phi(0)), \tag{12}$$

$$f'(\infty) \to 0, \theta(\infty) \to 0, \phi(\infty) = 0. \tag{13}$$

The physical quantities, skin friction, heat transfer rate and Sherwood number is defined by

$$C_f Re^{0.5} = 2\left((1+k)f''(0) - \frac{1}{3}\mathrm{K}\Lambda(f''(0))^3\right), \tag{14}$$

$$Nu_x Re_x^{-0.5} = -\left(1 + \frac{4}{3}Rd\right)\theta'(0), \tag{15}$$

$$Sh_x Re_x^{0.5} = -\phi'(0), \tag{16}$$

where

$$\Pr = \frac{\nu}{\alpha}, Q = \frac{\pi j_o M_o}{8\rho_l x a^2}, \beta = \frac{\pi}{b}\sqrt{\frac{\nu}{a}}, Rd = \frac{4\sigma^* T_\infty^3}{KK^*}, \mathrm{N}b = \frac{(\rho c)_p D_B\left(C_{np} - C_\infty\right)}{(\rho c)_l \nu}, K_1 = \frac{K_r^2}{a},$$
$$\mathrm{N}t = \frac{(\rho c)_p D_T(T_l - T_\infty)}{\nu(\rho c)_l T_\infty}, \Lambda = \frac{a^3x^3}{2\nu x C^{*2}}, \mathrm{K} = \frac{1}{\mu\gamma C^*}, Le = \frac{\alpha}{D_B}, \alpha_1 = \frac{h_1^*}{K}\sqrt{\frac{\nu}{a}}, \alpha_2 = \frac{h_2^*}{D_B}\sqrt{\frac{\nu}{a}},$$
$$L_1 = \lambda_1\sqrt{\frac{a}{\nu}}, \lambda = \frac{g\beta_1(T_w - T_\infty)}{a^2x}, \beta_t = \frac{\beta_2}{\beta_1}(T_w - T_\infty), \beta_c$$
$$= \frac{\beta_4}{\beta_3}\left(C_{np} - C_\infty\right), \mathrm{N}^* = \frac{\beta_3}{\beta_1}\left(\frac{C_{np} - C_\infty}{T_l - T_\infty}\right), E_1 = \frac{Ea}{KT_\infty}, \delta = \frac{T_l - T_\infty}{T_\infty}. \tag{17}$$

## 3. Numerical method

To perform numerical simulations, we use the Chebyshev collocation method [29]. The essence of this method is the set of Chebyshev polynomials. The Chebyshev polynomials form a sequence of orthogonal polynomials over the closed interval [−1, 1]. After the discretization of system of nonlinear ordinary differential equations, we solve the algebraic system of nonlinear equations by using Newton method with dumping. We also compared our results with the previous published data in ref. [27] (see Table 1).

## 4. Results and discussion

This segment of the article is dedicated to examine the influence of various fluid parameters on the flow profiles as shown in Figs. 1–14. The pertinent variables and constants that contribute mainly are dimensionless parameter $\beta$, fluid parameter $K$, Lewis number $Le$, modified Hartman factor $Q$, Brownian motion parameter $N_b$, Thermophoretic parameter $N_t$, radiation parameter $R_D$, Prandtl number $Pr$, second order slip parameter $L_1$, and Biot numbers $\alpha_1$ and $\alpha_2$, respectively.

Variation of $\beta$ are examined in Fig. 3. It is noted that by increasing the numerical values of dimensionless parameter brings more shear thinking effects to suspension. Therefore, the nanofluid is retarded with the increase $\beta$. Similarly, velocity of the suspension reduces subject to more lubrication at the edges of the Riga plate as shown in Fig. 4. The fluid particles close to the boundary of the channel find hard to get momentum due to slippage which results in vivid decline in the velocity by increasing slip parameter $L_1$. Fig. 4 shows the variation of fluid parameter on the velocity of nanofluid suspension. The diagram depicts that fluid gains extra momentum at the center of Riga plate when $K$ is increased numerically. This increase trend in the velocity can be attributed to shear thinning effects. Since, equation clearly describe that fluid parameter is inversely related to the viscosity of the base liquid. Therefore, grater fluid parameter, lesser the viscosity. Hence, faster the nanofluid flow. Whereas, the initial

**Table 1** Comparison with previous study.

| $\beta$ | Rasool and Zhang [17] | | Present | |
|---|---|---|---|---|
| | $Re_x^{-0.5}Nu_x$ | $Re_x^{-0.5}Sh_x$ | $Re_x^{-0.5}Nu_x$ | $Re_x^{-0.5}Sh_x$ |
| 0 | 0.3459 | 0.3469 | 0.3459 | 0.3469 |
| 0.5 | 0.3305 | 0.3363 | 0.3305 | 0.3363 |
| 1 | 0.3252 | 0.3327 | 0.3252 | 0.3327 |

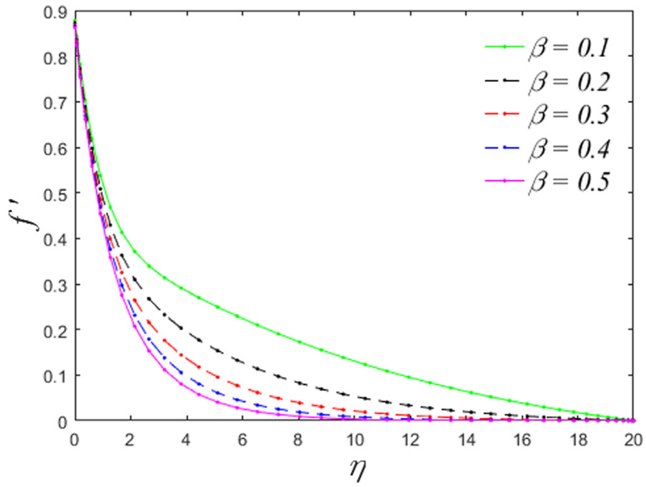


**Fig. 1** Effects of $\beta$ on velocity of the fluid.

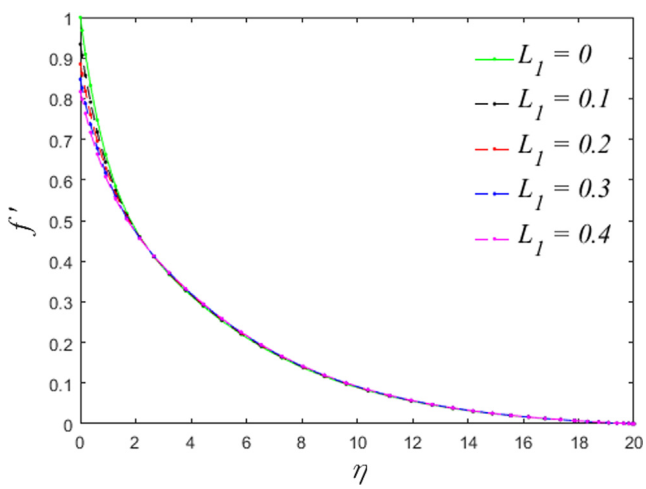


**Fig. 2** Effects of $L_1$ on the velocity of the fluid.

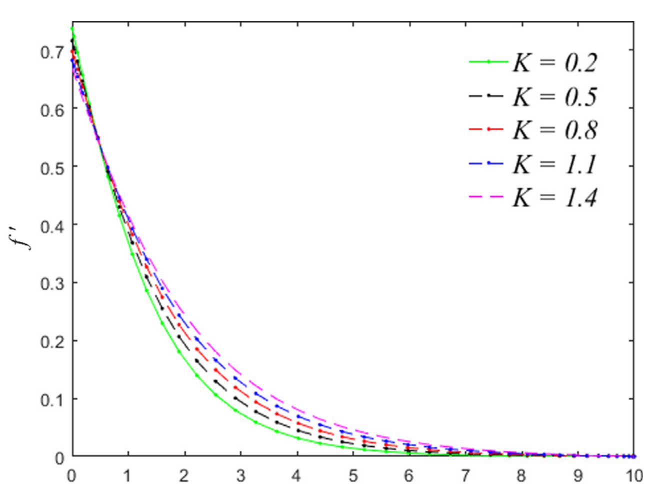


**Fig. 3** Effects of $K$ on velocity of the fluid.

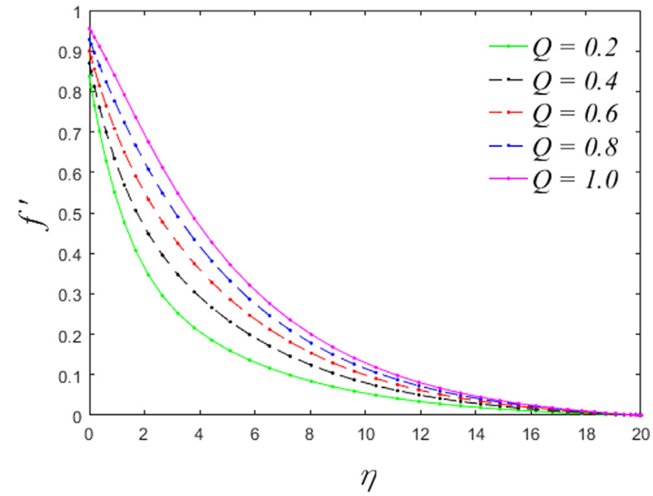


**Fig. 4** Effects of $Q$ on the velocity of the fluid.

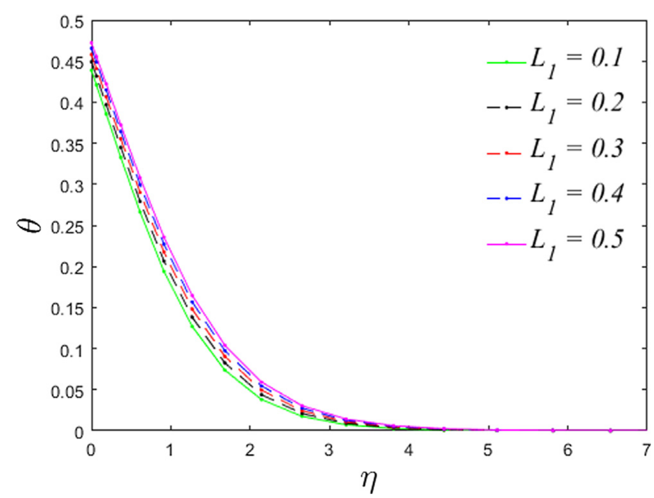


**Fig. 5** Effects of $L_1$ on temperature.

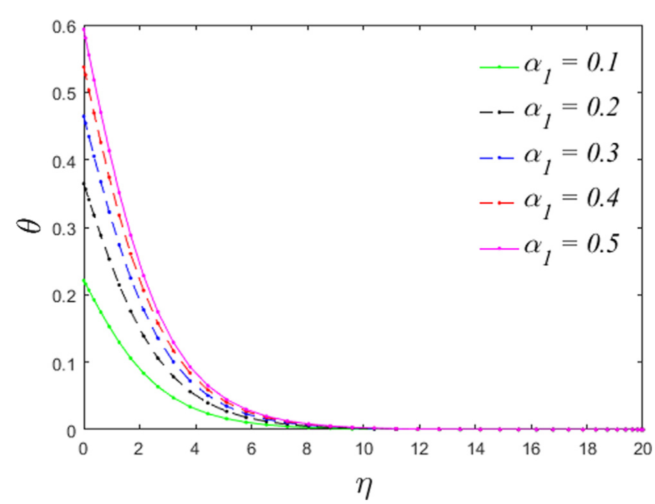


**Fig. 6** Effects of $\alpha_1$ on temperature.

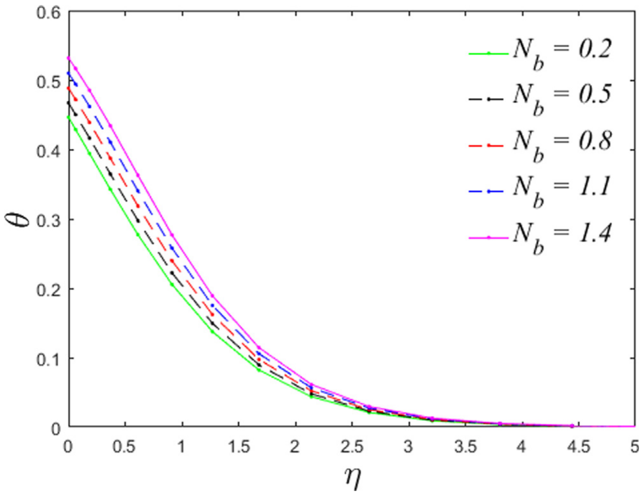


**Fig. 7** Effects of $N_b$ on temperature.

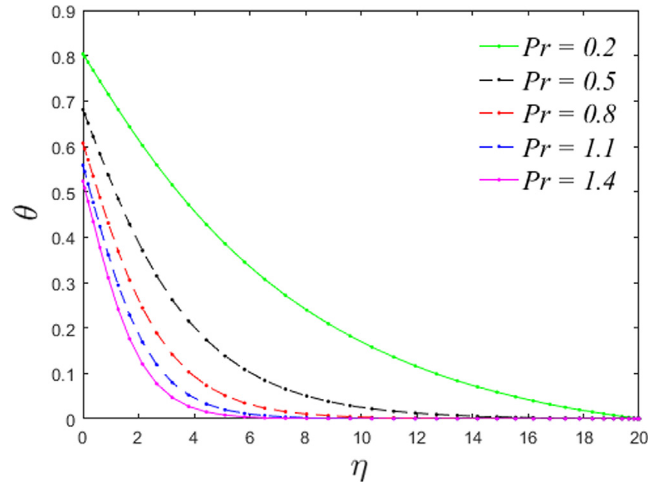


**Fig. 10** Effects of $Pr$ temperature.

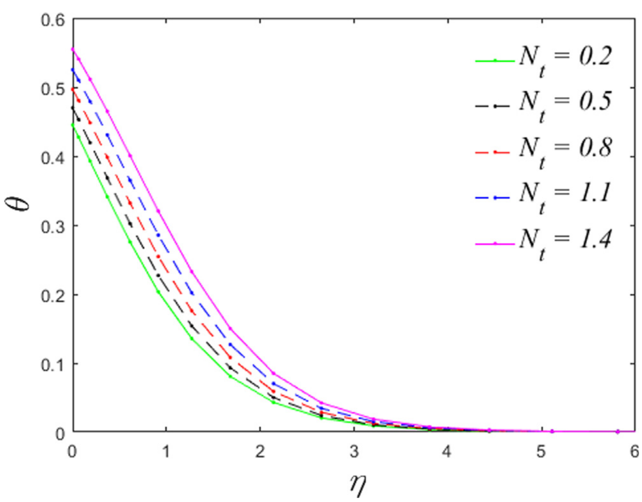


**Fig. 8** Effects of $N_t$ temperature.

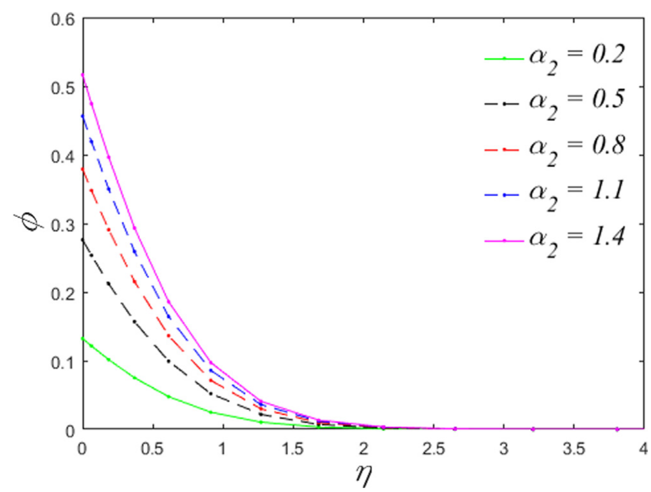


**Fig. 11** Effects of $\alpha_2$ on concentration of the particles.

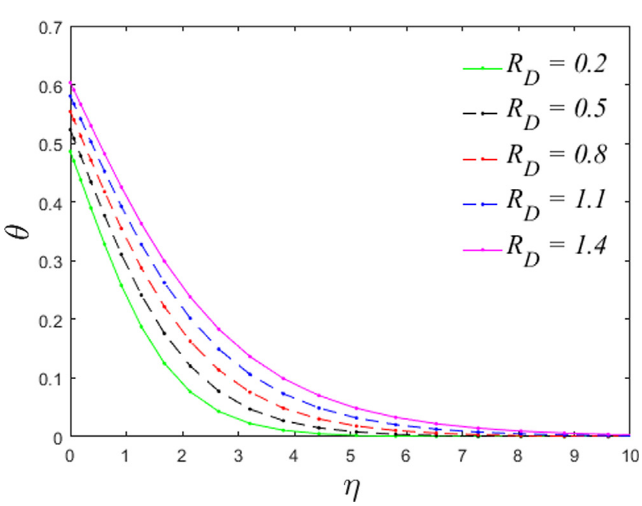


**Fig. 9** Effects of $R_D$ on temperature.

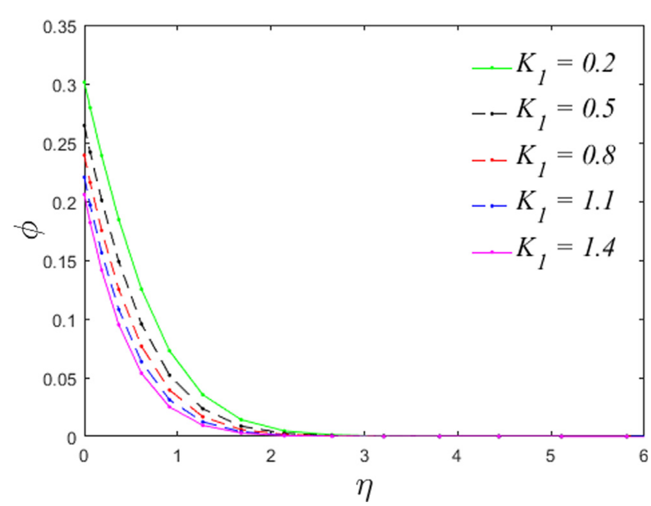


**Fig. 12** Effects of $K_1$ on concentration of the particles.

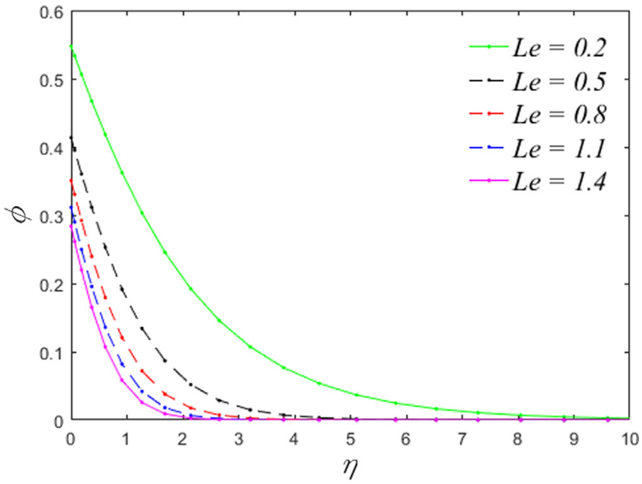


**Fig. 13** Effects of $Le$ on concentration of the particles.

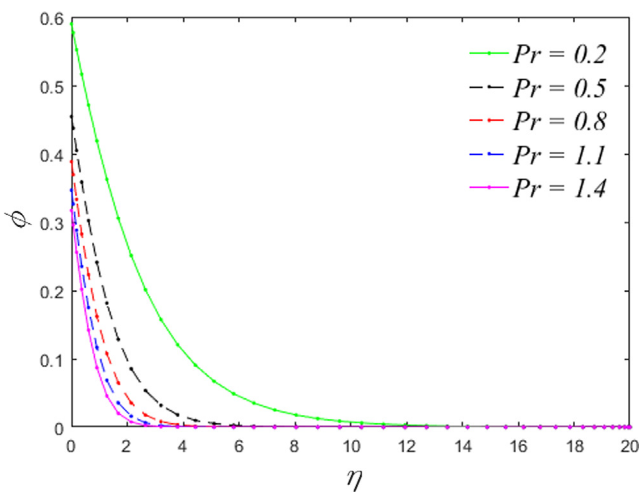


**Fig. 14** Effects of $Pr$ on concentration of the particles.

retardation indicates the application boundary slip condition. In the same way, momentum of the nanoflow also increase due to Hartmann factor in Fig. 5. The higher values of $Q$ accelerate the flow. This is important to know that Riga pate produces Lorentz force along the surface which ultimately introduces more surface tension to the system. Then this surface tension improves the momentum boundary layer of nanoflow.

Thermal profile of boundary layer with respect to various parameter is plotted in Figs. 5-10. More heat is added to the system in response to slip parameter. Since, $L_1$ resists the flow and force of friction between adjacent fluid particles gets enormous. Then more hear is generated. Therefore, thermal boundary layer starts bulging out in Fig. 5. Temperature profile also rises for $\alpha_1$ which can be witnessed in Fig. 6. The Biot factor aggravates the transport of heat and contribution of nanoparticles makes the convection, further strong. Therefore, temperature rises for $\alpha_1$. Fig. 7 shows the influence of $N_b$ on the heat transfer. Variation in Brownian motion parameter expedites the random motion of nanoparticles that allows them to persistently collide with one another. This mutual collision of particles releases energy and thermal profile rises in return. Moreover, thermal boundary layer thickness expands due to Thermophoretic parameter as observed in Fig. 8. By varying $N_t$ Thermophoretic force between the particles gets stronger which allow the heated nanoparticles to transmit heat form the region of high temperature to region of lower temperature. Consequently, thermal boundary layer thickness increases. Similar type of expansion in thermal energy results for $R_D$ in Fig. 9 which is because of strong heat source. On the contrary, thermal boundary layer reduces in size due to high Prandtl number. Physically, thermal conductivity of Powell-Eyring fluid reduces subject to increase in $Pr$, as seen in Fig. 10.

Concentration of nanoparticles is discussed in Figs. 11–14. Influence of Biot factor in nanoparticle concentration is examined in Fig. 11. It is to keep in mind that $\alpha_2$corresponds to strong convection of nanoparticles. The variation of the parameter intensifies the mass convection which contributes in the rise of concentration profile. Therefore, concentration of the particles is higher when Biot number is strong. This is the main cause of an increase in concentration of boundary layer thickness. However, an opposite behavior is observed in Figs. 12–14 in the concentration profile. Chemical reaction has a negative impact on mass convection. In Fig. 12 as chemical reaction is aggravated then mass convection of the particles reduces near the surface of Riga plate. This squashes the concentration boundary layer thickness. In the same way, the concentration of nanoparticles reduces subject to rise in Lewis number and Prandtl number in Fig. 13 and Fig. 14, respectively.

## 5. Numerical results and validation

Since, the current study is a numerical investigation of nanoflow through Riga plate. Numerical simulation is carried out with the help of *"Pseudo-spectral collocation method"* by developing numerical code by using MATLAB. Therefore, numerical data has also been computed expressed through graphs. Besides, the visual study that numerical results have been compiled and tabulated to analyze the behavior of different dimensionless quantities such as skin friction coefficient, Nusselt number and Sherwood number. Table 2 is constructed for drag force against different parameters. It is noted there is a prominent increase in the drag due to $K$ and $\lambda$. On the other hand, drag force coefficient declines subject to $L_1$, $\Lambda$ and $Q$, respectively. Variation in heat flux against significant parameters is accumulated in Table 3. The data presented shows that Nusselt number is an increasing function of Prandtl number, radiation parameter and Biot factor respectively. Whereas, it decreases as Brownian motion parameter and Thermophoretic parameter are increased. Mass flux at different points of the domain are compiled in Table 4. The dimensionless number is inversely proportional to activation energy. On the contrary, Sherwood number increases in response to the variated parameters.

**Table 2** Variation of skin friction coefficient.

| $K$ | $L_1$ | $\Lambda$ | $Q$ | $\lambda$ | $-Re_x^{0.5}C_f$ |
|---|---|---|---|---|---|
| 0 | 0.5 | 1.0 | 0.3 | 0.1 | 0.8478 |
| 0.5 | | | | | 0.9665 |
| 1.0 | | | | | 1.0580 |
| 0.3 | 0.0 | | | | 1.7240 |
| | 0.2 | | | | 1.2107 |
| | 0.5 | | | | 0.9405 |
| | 0.25 | 0.0 | | | 1.1802 |
| | | 0.5 | | | 1.1781 |
| | | 1.0 | | | 1.1759 |
| | | 0.25 | 0.5 | | 0.9141 |
| | | | 0.8 | | 0.5512 |
| | | | 1.0 | | 0.3250 |
| | | | 0.25 | 0.0 | 1.2179 |
| | | | | 0.1 | 1.2498 |
| | | | | 0.15 | 1.3032 |

**Table 3** Variation of Nusselt Number.

| $N_b$ | $N_t$ | $Pr$ | $R_D$ | $\alpha_1$ | $Re_x^{0.5}Nu_x$ |
|---|---|---|---|---|---|
| 0.5 | 0.3 | 2.0 | 0.3 | 0.5 | 0.3612 |
| 1.0 | | | | | 0.3406 |
| 1.5 | | | | | 0.3198 |
| 0.3 | 0.5 | | | | 0.3570 |
| | 1.0 | | | | 0.3239 |
| | 1.5 | | | | 0.2886 |
| | 0.3 | 0.5 | | | 0.2296 |
| | | 0.8 | | | 0.2798 |
| | | 1.0 | | | 0.3031 |
| | | 2.0 | 0.5 | | 0.4216 |
| | | | 1.0 | | 0.5376 |
| | | | 1.5 | | 0.6371 |
| | | | 0.4 | 0.1 | 0.1304 |
| | | | | 0.4 | 0.3523 |
| | | | | 0.7 | 0.4601 |

**Table 4** Variation of Sherwood number.

| $Le$ | $k_1$ | $\alpha_2$ | $E_1$ | $n$ | $Re_x^{0.5}Sh_x$ |
|---|---|---|---|---|---|
| 0 | 0.5 | 0.3 | 0.3 | 0.5 | 0.2012 |
| 0.5 | | | | | 0.2240 |
| 1.0 | | | | | 0.2355 |
| 0.3 | 0.0 | | | | 0.1524 |
| | 0.5 | | | | 0.1821 |
| | 1.0 | | | | 0.1975 |
| | 0.25 | 0.1 | | | 0.0797 |
| | | 0.2 | | | 0.1326 |
| | | 0.3 | | | 0.1703 |
| | | 0.15 | 0.0 | | 0.1104 |
| | | | 0.25 | | 0.1089 |
| | | | 0.5 | | 0.1076 |
| | | | 0.15 | 0.0 | 0.1074 |
| | | | | 0.5 | 0.1076 |
| | | | | 1.0 | 0.1077 |

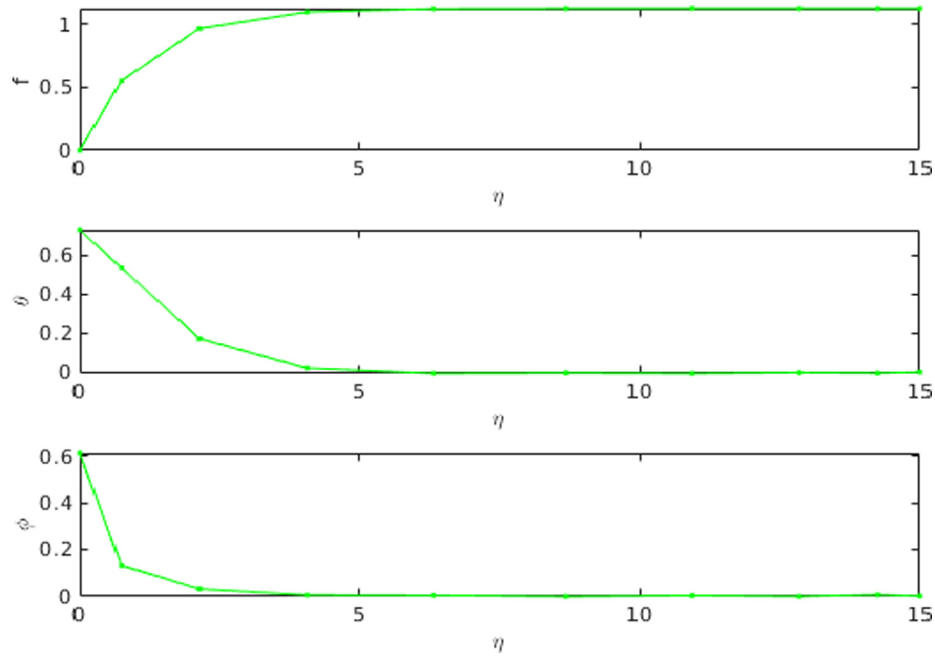


**Fig. 15** Profiles of $f, \theta$ and $\phi$ for $n = 10$ gird-points. The vector of zeros is taken as initial guess for dumped Newton method.

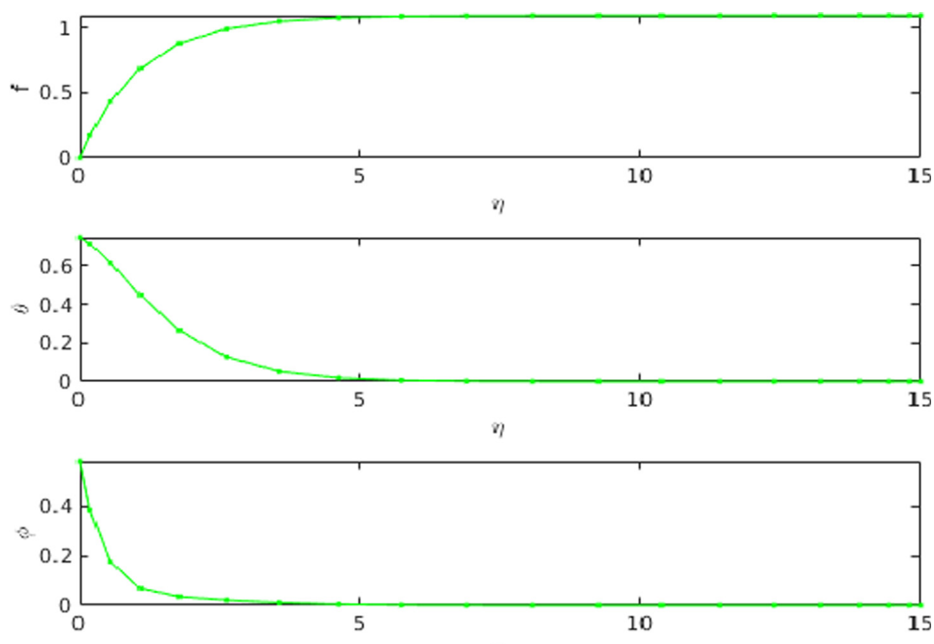


**Fig. 16** Profiles of $f, \theta$ and $\phi$ for $n = 20$ gird-points. The vector of zeros is taken as initial guess for dumped Newton method.

## 6. Convergence criteria and accuracy of the numerical results

For the grid-convergence, we first take $n = 10$ grid-points and solve the system of nonlinear equations by using dumped Newton method. In this case we take the initial guess zero vector and dumping factor was 0:001. The stopping criteria for the dumped Newton method is $1.0 \times 10^{-5}$in all numerical simulations. Fig. 15 shows the profiles of $f$and $\theta$ for $n = 10$. By observing Figs. 16–19, we can say that as we increase the number of grid-points we have the convergence in the numerical solution.

## 7. Conclusion

This a numerical investigation of nanofluid flow. Eyring-Powell fluid model is used as the base liquid. The mixed con-

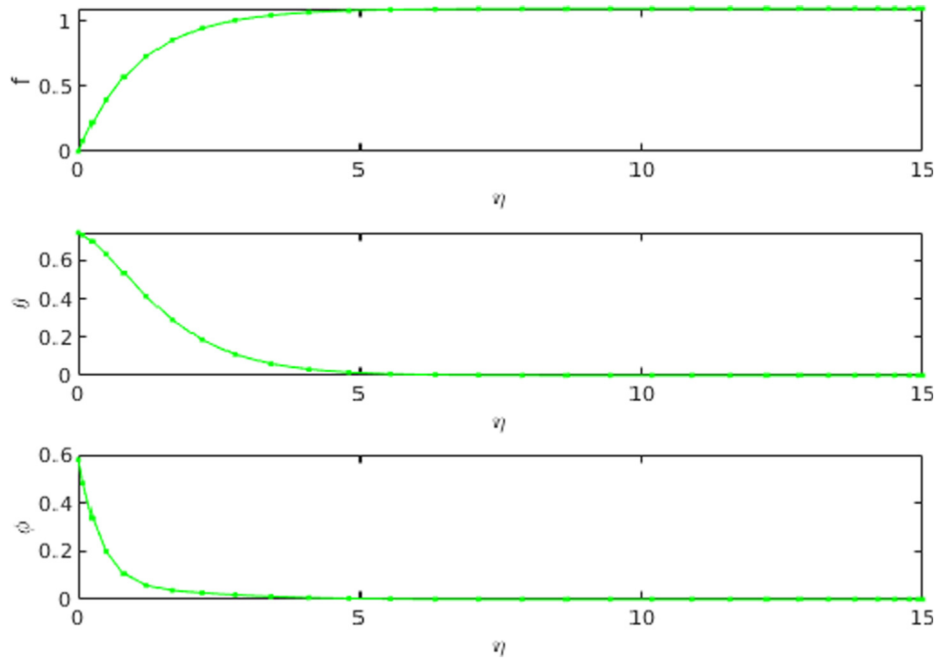


**Fig. 17** Profiles of $f, \theta$ and $\phi$ for $n = 30$ gird-points. The vector of zeros is taken as initial guess for dumped Newton method.

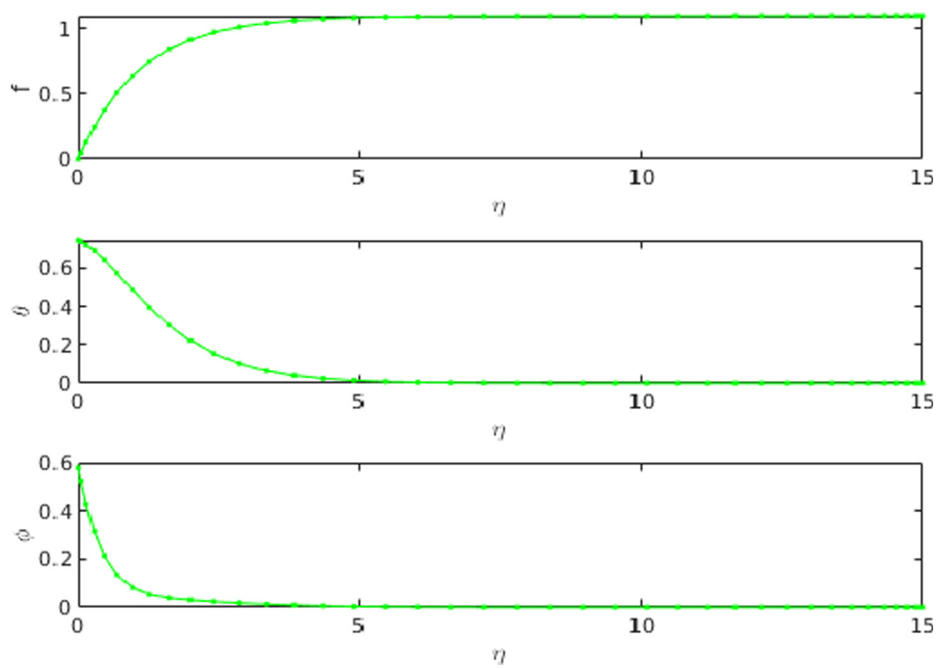


**Fig. 18** Profiles of $f, \theta$ and $\phi$ for $n = 40$ gird-points. The vector of zeros is taken as initial guess for dumped Newton method.

vection fluid flow through radiative Riga plate comes under the effects of activation energy and viscous dissipation. Second order slip condition are applied to add lubrication effects. Mathematical modeled partial differential equations are converted into a set of ordinary differential equations with the help of symmetry transformation method. The pseudo-spectral collocation method is picked and developed a MATLAB code to solve the system of nonlinear complex ordinary differential equations. A detailed parametric study is performed that highlight the following most prominent features:

[6] Velocity of nanofluid reduces due to lubricated walls of the Riga whereas, thermal boundary thickness increases.
[6] Radom motion of nanoparticles contribute to extra energy to the system.
[6] Due to thermophoretic force heated tiny particles transmit form higher region of concentration to lower region of concentration.
[6] Prandtl number has an analogous effect on heat flux and as well as, mass flux.

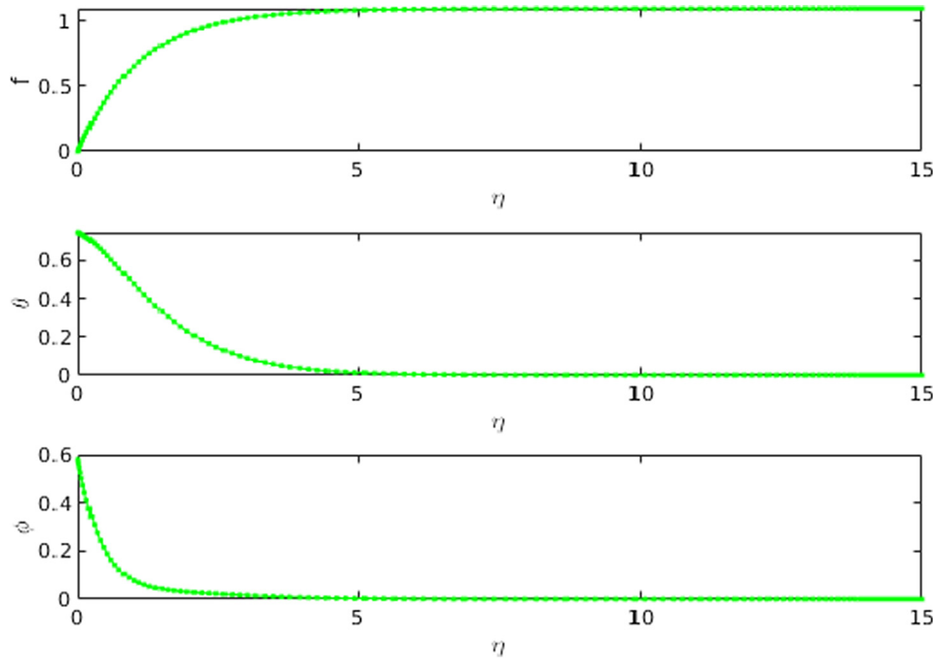


**Fig. 19** Profiles of $f, \theta$ and $\phi$ for $n = 130$ gird-points. The vector of zeros is taken as initial guess for dumped Newton method.

[6] Each profile approaches the free stream values asymptotically.

## Declaration of Competing Interest

The authors declare that they have no known competing financial interests or personal relationships that could have appeared to influence the work reported in this paper.

## Acknowledgments

The research was supported by the National Natural Science Foundation of China (Grant Nos. 11971142, 11871202, 61673169, 11701176, 11626101, 11601485).

## References

[1] M. Nazeer, N. Ali, F. Ahmad, M. Latif, Numerical and perturbation solutions of third-grade fluid in a porous channel: Boundary and thermal slip effects, Pramana – J. Phys. 94 (2020) 44.
[2] M.I. Khan, M. Waqas, T. Hayat, A. Alsaedi, A comparative study of Casson fluid with homogeneous-heterogeneous reactions, J. Colloid Interface Sci. 498 (2017) 85–90.
[3] A.J. Chamkha, R.A. Mohamed, S.E. Ahmed, Unsteady MHD natural convection from a heated vertical porous plate in a micropolar fluid with Joule heating, chemical reaction and radiation effects, Meccanica 46 (2011) 399–411.
[4] M.I. Khan, S. Qayyum, T. Hayat, M.I. Khan, A. Alsaedi, T.A. Khan, Entropy generation in radiative motion of tangent hyperbolic nanofluid in presence of activation energy and nonlinear mixed convection, Phys. Lett. A 382 (2018) 2017–2026.
[5] R.A. Damseh, M.Q. Al-Odata, A.J. Chamkha, B.A. Shannak, Combined effect of heat generation or absorption and first-order chemical reaction on micropolar fluid flows over a uniformly stretched permeable surface, Int. J. Therm. Sci. 48 (2009) 1658–1663.
[6] M. Nazeer, N. Ali, T. Javed, M. Razzaq, Finite element analysis of bi-viscosity fluid enclosed in a triangular cavity under thermal and magnetic effects, Eur. Phys. J. Plus (EPJP) 2 (2019) 134.
[7] E. Magyari, A.J. Chamkha, Combined effect of heat generation or absorption and first-order chemical reaction on micropolar fluid flows over a uniformly stretched permeable surface: The full analytical solution, Int. J. Therm. Sci. 49 (2010) 1821–1828.
[8] M.I. Khan, F. Alzahrani, A. Hobiny, Heat transport and nonlinear mixed convective nanomaterial slip flow of Walter-B fluid containing gyrotactic microorganisms, Alexandria Eng. J. 59 (2020) 1761–1769.
[9] S.O. Salawu, A.R. Hassan, A. Abolarinwa, N.K. Oladejo, Thermal stability and entropy generation of unsteady reactive hydromagnetic Powell-Eyring fluid with variable electrical and thermal conductivities, Alexandria Eng. J. 58 (2019) 519–529.
[10] M.I. Khan, F. Alzahrani, A. Hobiny, Z. Ali, Estimation of entropy optimization in Darcy-Forchheimer flow of Carreau-Yasuda fluid (non-Newtonian) with first order velocity slip, Alexandria Eng. J. 59 (2020) 3953–3962.
[11] N. Ali, F. Nazeer, M. Nazeer, Flow and heat transfer of Eyring-powell fluid in a pipe, Zeitschrift für Naturforschung A (ZNA) 73 (3) (2018) 265–274.
[12] R. Muhammad, M.I. Khan, N.B. Khan, M. Jameel, Magnetohydrodynamics (MHD) radiated nanomaterial viscous material flow by a curved surface with second order slip and entropy generation, Comput. Methods Programs Biomed. 189 (2020) 105294.
[13] M. Nazeer, F. Ahmed, M. Saeed, A. Saleem, S. Naveed, Z. Akram, Numerical solution for flow of a Eyring-powell fluid in a pipe with prescribed surface temperature, J. Braz. Soc. Mech. Sci. Eng. 41 (2019) 518.
[14] R. Muhammad, M.I. Khan, M. Jameel, N.B. Khan, Fully developed Darcy-Forchheimer mixed convective flow over a curved surface with activation energy and entropy generation, Comput. Methods Programs Biomed. 188 (2020) 105298.
[15] D. Kumar, K. Ramesh, S. Chandok, Mathematical modeling and simulation for the flow of magneto-Powell-Eyring fluid in

an annulus with concentric rotating cylinders, Chin. J. Phys. 65 (2020) 187–197.
[16] S.H. Seyedi, B.N. Saray, A.J. Chamkha, Heat and mass transfer investigation of MHD Eyring-Powell flow in a stretching channel with chemical reactions, Phys. A 544 (2020) 124109.
[17] G. Rasool, T. Zhang, Characteristics of chemical reaction and convective boundary conditions in Powell-Eyring nanofluid flow along a radiative Riga plate, Heliyon 5 (4) (2019) e01479.
[18] M.M. Bhatti, T. Abbas, M.M. Rashidi, Effects of thermal radiation and electromagnetohydrodynamics on viscous nanofluid through a Riga plate, Multidisc. Model. Mater. Struct. 12 (4) (2016) 605–618.
[19] A. Gailitis, O. Lielausis, On a possibility to reduce the hydrodynamic resistance of a plate in an electrolyte, Appl. Mag. Rep. Phys. Inst 12 (1) (1961) 143–146.
[20] M.M. Bhatti, T. Abbas, T.T. Rashidi, Entropy generation as a practical tool of optimization for non-Newtonian nanofluid flow through a permeable stretching surface using SLM, J. Comput. Des. Eng. 4 (2017) 21–28.
[21] T. Abbas, T. Hayat, M. Ayub, M.M. Bhatti, A. Alsaedi, Electromagnetohydrodynamic nanofluid flow past a porous Riga plate containing gyrotactic microorganism, Neural Comput. Appl. 31 (2019) 1905–1913.
[22] T. Abbas, M. Ayub, M.M. Bhatti, M.M. Rashidi, A. Alsaedi, Entropy generation on nanofluid flow through a horizontal riga plate, Entropy 18 (2016) 223.
[23] M.I. Khan, F. Alzahrani, Free convection and radiation effects in nanofluid (Silicon dioxide and Molybdenum disulfide) with second order velocity slip, entropy generation, Darcy-Forchheimer porous medium, Int. J. Hydrogen Energy, (2020) In press.
[24] T. Hayat, S. Qayyum, M. Imtiaz, A. Alseadi, Comparative study of silver and copper water nanofluids with mixed convection and nonlinear thermal radiation, Int. J. Heat Mass Transf. 102 (2016) 723–732.
[25] M.K. Nayak, S. Shaw, M.I. Khan, V.S. Pandey, M. Nazeer, Flow and thermal analysis on Darcy-Forchheimer flow of copper-water nanofluid due to a rotating disk: A static and dynamic approach, J. Mater. Res. Technol. 9 (2020) 7387–7408.
[26] M.V. Krishna, A.J. Chamkha, Hall and ion slip effects on MHD rotating boundary layer flow of nanofluid past an infinite vertical plate embedded in a porous medium, Results Phys. 15 (2019) 102652.
[27] M.V. Krishna, A.J. Chamkha, Hall and ion slip effects on MHD rotating flow of elastico-viscous fluid through porous medium, Int. Commun. Heat Mass Transfer 113 (2020) 104494.
[28] A.J. Chamkha, A. Doostanidezfuli, E. Izadpanahi, M. Ghalambaz, Phase-change heat transfer of single/hybrid nanoparticles-enhanced phase-change materials over a heated horizontal cylinder confined in a square cavity, Adv. Powder Technol. 18 (2) (2017) 385–397.
[29] F. Ahmad, E. Tohidi, J.A. Carrasco, A parameterized multi-step Newton method for solving systems of nonlinear equations, Numer. Algorithms 71 (2016) 631–653.